Stan ZUREK

Megger Instruments Ltd, Archcliffe Road, Dover, CT17 9EN, United Kingdom

doi:10.15199/48.2017.07.04

Example of vanishing anisotropy at high rotational magnetisation of grain-oriented electrical steel

Abstract. *This paper presents experimental data measured up to 2T under rotational circular flux density. The results show that at lower excitations there is significant anisotropy of permeability. However at 2T the anisotropy collapses so that the permeability varies only ±14% from the average value. On a qualitative level the results are very similar to the directional curves for single-crystal samples for the three significant crystallographic directions [100], [110] and [111] shown previously in the literature.*

Streszczenie. *Artykuł prezentuje dane eksperymentalne do amplitudy 2 T przy przemangesowaniu obrotowym kołowym. Rezultaty pokazują, że przy mniejszym wymuszeniu występuje znacząca anizotropia przenikalności. Jednak przy 2T anisotropia zanika i przenikalność zmienia się tylko o ±14% w porównaniu do wartości średniej. W ujęciu jakościowym wyniki są bardzo podobne do krzywych kierunkowych dla monokryształu dla trzech głównych kierunków [100], [110] i [111] zgodnie z poprzednimi publikacjami. (**Przykład zanikającej anizotropii orientowanej blachy elektrotechnicznej przy przemagnesowaniu obrotowym od dużej amplitudzie**).*

Keywords: rotational magnetisation, anisotropy, electrical steel.
Słowa kluczowe: przemagnesowanie obrotowe, anizotropia, blacha elektrotechniczna.

1. Introduction

Grain-oriented electrical steels (GO) are materials commonly used for magnetic cores of transformers and other electric machines. GO exhibit high anisotropy of magnetic properties due to their crystallographic structure.

A cubic crystallite has a shape for which the planes and directions can be defined as shown in Fig. 1. The alignment of crystallites in each grain is controlled during production so that one "easy" magnetisation direction is produced [1]. In this so-called Goss structure (from the name of its inventor [2]) the crystallites are aligned in such a way that all three important crystallographic directions are located within the plane of the sheet (Fig. 1).

The "easy" direction is along the rolling direction (RD) and it caused by all the crystallites having their [100] directions aligned with it. The direction [110] is the face diagonal (Fig. 1a) and is in the transverse direction (TD, perpendicular to RD). The direction [111] is the cube diagonal.

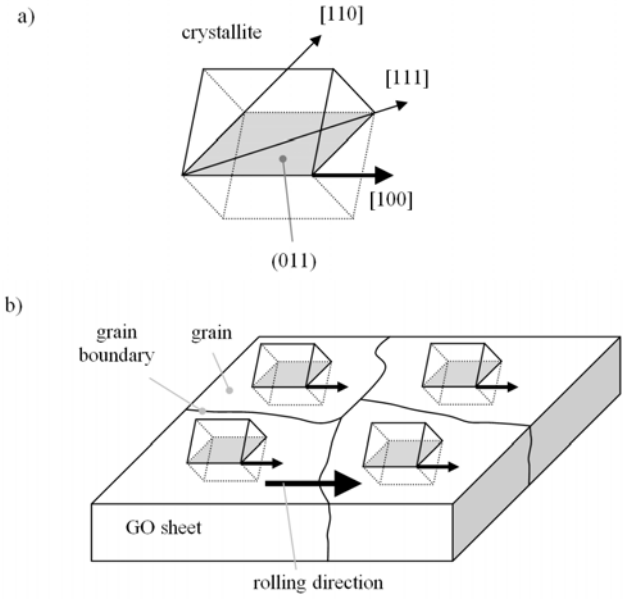

Fig.1. Goss structure in GO: a) directions in a crystallite, b) alignment of crystallites in GO sheet [3,4]

B-H curves measured for the three crystallographic directions for a single crystal are shown in Fig. 2 [1,3 4]. At lower excitations, within practically applicable range, the [100] direction (0° with respect to RD) has the highest permeability. The [110] direction (90° with respect to RD) has significantly lower permeability, and [111] has the lowest permeability (55° with respect to RD).

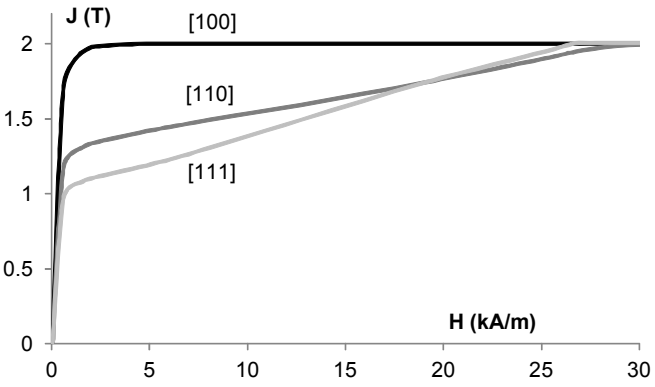

Fig.2. Directional *B-H* characteristics of a single-crystal material; adapted from [1]

However, all the directions have the same value of polarisation saturation, which for single-crystal material requires at least 30 kA/m (Fig. 2). A single-crystal material is an "ideal" material in which the whole volume is occupied by a single grain, rather than by multiple grains (each of which can be slightly misaligned) shown in Fig. 1b.

The directional properties shown in Fig. 2 were measured by cutting special samples at specific angles. The excitation was applied in an alternating manner, for instance in Epstein frame [5].

2. Rotational magnetisation

Rotational magnetisation occurs in magnetic cores of three-phase electric machines such as motors, generators and also T-joints of transformers [6, 7].

Rotational magnetisation can be reproduced in the laboratory, for example by means of magnetising yoke shown in Fig. 3. The yoke can be made in a similar shape as a motor stator, wound with two-phase winding. The phases are orthogonal: one magnetises in X direction, the other in the Y direction.

Fig.3. Two-phase yoke for rotational magnetisation of a single-sheet sample [7]

The sample is in a form of a single circular disk placed inside the yoke. Rotating magnetic field is set up in the yoke when the two phases are energised (with 90° phase shift). The excitation can be controlled with a digital feedback [8,9] so that given magnetising conditions can be precisely set.

For example, it is possible to generate circular flux density *B* (circular loci of the *B* vector) even though the crystallographic directions have significantly different magnetic properties (Fig. 2). The circular *B* is obtained by ensuring that a vector of a fixed magnitude is rotated at constant speed within the plane of lamination (Fig. 4) [7].

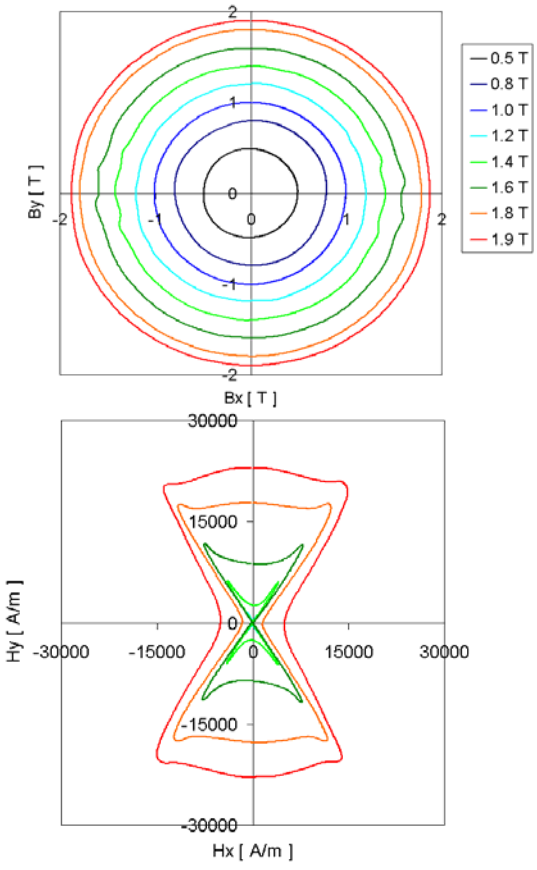

Fig.4. Typical results measured under controlled circular B (top) with corresponding H loci (bottom) for typical GO, at 50 Hz [7]

In order to achieve such conditions, due to the anisotropy of permeability, the magnetic field strength *H* must vary accordingly within each cycle of rotation.

As a result a typical "butterfly" *H* loci is generated. It is evident from Fig. 4 that the RD of the sample is synonymous with the horizontal axis of the H loci graph, because at lower excitations it required the lowest *H* to obtain the same *B*, so the permeability was highest (compare with Fig. 2).

3. Results at very high flux density

According to the curves shown in Fig. 2 at sufficiently high excitation the material should saturate. This corresponds to conditions in which for each direction permeability will be the same or similar – thus the anisotropy of permeability should vanish, or at least be significantly reduced.

Rotational measurements under controlled *B* rotation are quite difficult to carry out in practice, especially at high *B*. Values above 1.9 T required using an especially adjusted rotational magnetisation system with two power amplifiers for the magnetising phase working in the TD direction [7], and a third power amplifier for the RD direction.

The results are shown in Fig. 5 and Fig. 6. Only data for 1.7 T and above are shown, because for lower excitation the behaviour is well known, as shown for instance in Fig. 4.

The *B* loci (Fig. 5, top) remain circular because this was the controlled quantity. There are some minor distortions visible as the circular shape passes through the horizontal axis. This was caused by limited resolution of the feedback control due to very fast changes of the *H* vector passing through RD.

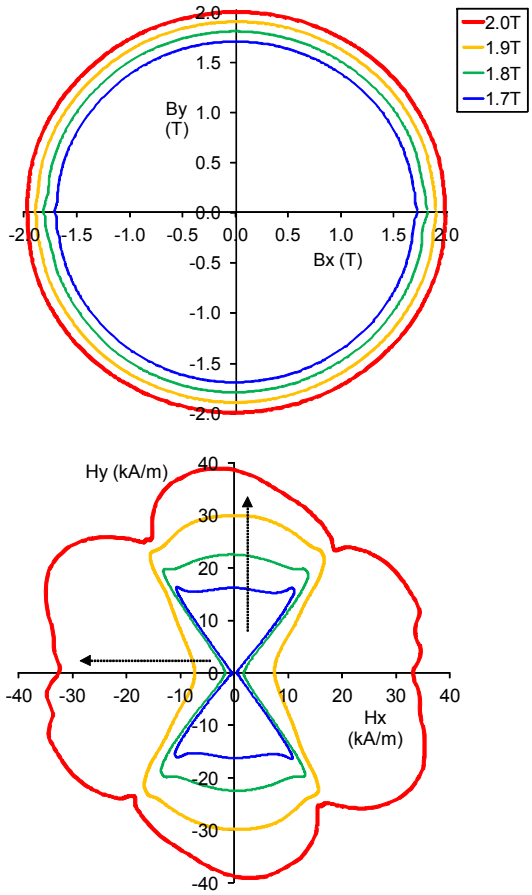

Fig.5. Rotational results for conventional grain-oriented electrical steel M089-27N, at 50 Hz

Interesting behaviour occurs above 1.8 T (Fig. 5, bottom). At 1.9 T the *H* loci begins to significantly "swell" in all directions, including TD and RD. And at 2.0 T the H loci loses its original "butterfly" shape and develops into a shape whose instantaneous radius varies much less than for lower excitations.

The corresponding directional permeability curves are shown in Fig. 6. At 0° and 180° the *B* vector passes through RD or the "easy" direction so permeability is high. At 1.7 T permeability is lowest at around 55° (and other corresponding symmetrical directions: 125°, 235° and 305°), which is noticeably lower than at 90°. This corresponds well with the curves shown in Fig. 2.

It should be noted that it was required to generate in excess of 30 kA/m in order to reach 2.0 T in all directions, as evident from Fig. 5 (bottom). This is also supported by the curves from Fig. 2. At such excitation the anisotropy of permeability reduces to rather small variation, changing only from relative amplitude permeability μ_r = 40.0 to 53.6. Therefore the change is only ±14% from the average value through the whole rotation. Whereas at 1.9 T permeability changes from μ_r = 50.4 to 204, or up to +172% from the average value. At lower excitation the variation, hence anisotropy is even greater.

The excitation at 2.0 T is still far from full saturation, for which by definition it would have to be μ_r = 1. However, it can be observed from Fig. 6 that at 2.0 T around 55° (and 125°, 235°, 305°) the instantaneous permeability is higher than at 90° (and 270°). Again, this is supported by the curves in Fig. 2, in which between 20-30 kA/m the [111] curve overtakes the [110] curve.

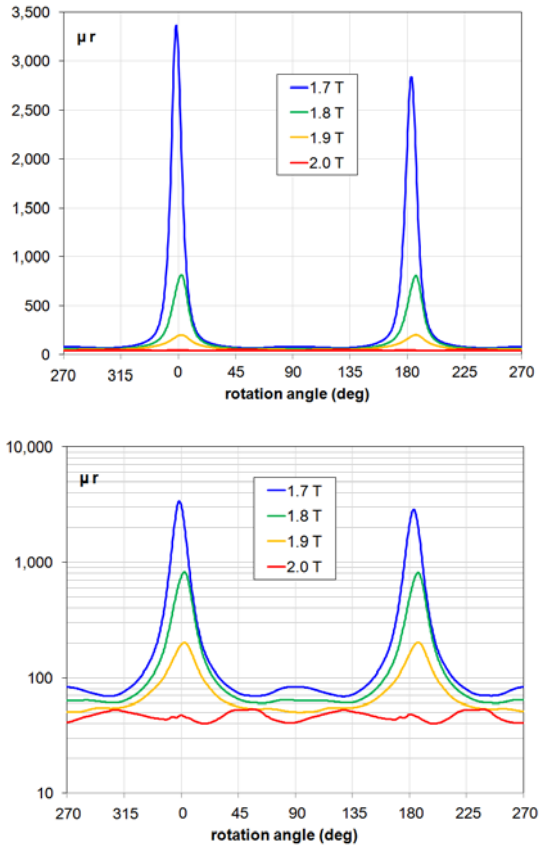

Fig.6. Permeability vs. rotation angle for data from Fig. 5, the same data is presented with linear vertical scale (top) and logarithmic vertical scale (bottom)

4. Summary

The results presented in Fig. 5 and Fig. 6 for 2.0 T excitation were very difficult to obtain with the apparatus and it was not possible to repeat them at different frequency or different sample. Results up to 1.9 T were possible for different samples (Fig. 4), but the level of excitation was insufficient to attain significant reduction in the anisotropy of permeability.

Nevertheless, it can be observed that in Fig. 4 similar "swelling" of the *H* loci begins to take place at 1.9 T. On the qualitative level the curve at 1.9 T from Fig. 4 and 1.9 T from Fig. 5 display very similar shape and characteristics.

It should be noted that the data in Fig. 5 is based on the measurement of *B* and not *J* as in Fig. 2. In the given setup (Fig. 3) it was not possible to use the air flux compensation. At 30 kA/m the $\mu_0 \cdot H$ component is equal to 37.7 mT, which is around 1.9% of the 2.0 T amplitude. Such error probably contributed in an adverse way to the control of circular *B* shape and it is possible that some asymmetry visible in the "lobes" in the *H* loci for the highest excitation are related to such artefact, especially that curves only for anticlockwise rotation are shown.

Another detail which can be observed from Fig. 6 is that the peaks of the μ_r curves do not fall ideally at 0° and 180°. This could be attributed to finite resolution of the feedback algorithm, which had to cope with large variation of the permeability through the rolling direction.

However, the presented data shows that the anisotropy of permeability collapses at very high excitation, showing behaviour very similar to the single-crystal samples.

***Author**: Dr Stan Zurek, Megger Instruments Ltd, Archcliffe Road, Dover, CT17 9EN, United Kingdom E-mail: Stan.Zurek@ieee.org*

REFERENCES

[1] Beckley P., Electrical steels, *European Electrical Steels*, Newport, UK, 2000

[2] Goss N.P., Electrical sheet and method and apparatus for its manufacture and test, *US Patent* 1,965,559, 1934

[3] Soinski M., Magnetic materials in technology, (in Polish: Materiały magnetyczne w technice), *Centralny Ośrodek Szkolenia i Wydawnictw SEP*, 2001

[4] Tumanski S., Handbook of magnetic measurements, *CRC Press*, 2011

[5] IEC 60404-2:1998 (Epstein frame)

[6] Zurek S., et al., Rotational power losses and vector loci under controlled high flux density and magnetic field in electrical steel sheets, *IEEE Trans. Magnetics*, Vol. 42 (10), 2006, p. 2815

[7] Zurek S., Two-dimensional magnetisation problems in electrical steels, PhD thesis, *Wolfson Centre for Magnetics Technology*, Cardiff University, Cardiff, United Kingdom, 2005

[8] Zurek S., et al., Use of novel adaptive digital feedback for magnetic measurements under controlled magnetising conditions, *IEEE Trans. Magnetics*, Vol. 41 (11), 2005, p. 4242

[9] Zurek S., Practical implementation of universal digital feedback for characterisation of soft magnetic materials under controlled ac waveforms, presented at *Symposium of Magnetic Measurements & Modeling*, Czestochowa – Siewierz, Poland, 2016